Deep subwavelength nanolithography using localized surface plasmon modes on planar silver mask

W. Srituravanich, S. Durant, H. Lee, C. Sun, and X. Zhang

Deep subwavelength nanolithography using localized surface plasmon modes on planar silver mask

W. Srituravanich, S. Durant, H. Lee, C. Sun, and X. Zhang[a]

NSF Nano-scale Science and Engineering Center (NSEC), 5130 Etcheverry Hall, University of California, Berkeley, California 94720-1740

The development of a near-field optical lithography is presented in this paper. By accessing short modal wavelengths of localized surface plasmon modes on a planar metallic mask, the resolution can be significantly increased while using conventional UV light source. Taking into account the real material properties, numerical studies indicate that the ultimate lithographic resolution at 20 nm is achievable through a silver mask by using 365 nm wavelength light. The surface quality of the silver mask is improved by adding an adhesion layer of titanium during the mask fabrication. Using a two-dimensional hole array silver mask, we experimentally demonstrated nanolithography with half-pitch resolution down to 60 nm, far beyond the resolution limit of conventional lithography using *I*-line (365 nm) wavelength. © *2005 American Vacuum Society.* [DOI: 10.1116/1.2091088]

I. INTRODUCTION

Due to the diffractive nature of the light, the resolution of conventional optical lithography is limited to the wavelength of the illumination light. According to Abbe's theory, the resolution can be improved by using either shorter wavelengths or higher numerical apertures. Although the semiconductor industry has made significant progress in increasing the lithography resolution in the past decades, further improvement of the resolution by accessing shorter wavelengths is facing critical challenges due to the availability of suitable optical materials.[1] Yet, efforts in using the high numerical apertures are constrained by the highest refractive index being available from the nature materials. While Abbe's theory describes the limit of optical resolution at the far field, people soon realized the high optical resolution can be practically obtained at the near field. By collecting the evanescent waves at the near field, several near-field optical lithographies[2] have been developed with the resolution beyond the diffraction limit while using near-UV or visible wavelength light sources. However, due to the nature of the exponential decay of evanescent waves through subwavelength structures, the optical intensity is strongly attenuated. Thus, the low optical throughput limits practical application of such lithography methods. To solve this problem, the transmitted optical field needs to be strongly amplified. Fortunately, the surface plasmon resonance effect offers a unique solution to solve this problem. In plasmonic lithography,[3] the evanescent field is strongly enhanced using the resonant excitation of surface plasmons that can be excited at given conditions. However, the resolution is limited by the surface plasmon wavelengths. In our previous study, an effort to utilize ultrashort modal wavelengths of surface plasmons has been proposed.[4] The numerical simulations suggested that, using a silver mask, an optical lithography down to 30 nm could be achieved, and a preliminary lithog-

raphy result of features as small as 100 nm on a periodicity of 200 nm has been demonstrated. However, due to the challenges in mask fabrication at such a small scale, the experimental results at this resolution were not provided at that time.

In this paper, we present the study of the high-resolution plasmonic lithography to further understand the underlying physics along with the experimental demonstrations. We investigate the resolution limit of the proposed nanolithography method both through analytical and numerical studies. Concurrently, we are optimizing the fabrication process to improve the quality of the plasmonic mask. Finally, we conduct a lithography experiment using a two-dimensional (2-D) nanohole array silver mask to confirm the theoretical prediction.

II. PRINCIPLE AND NUMERICAL MODELING

Surface plasmons (SPs) are the collective electron oscillations at the interface between a metal and an insulator. SPs have become very attractive among the scientific community after being introduced as the underlying mechanism of the extraordinary transmission through subwavelength holes on an opaque metal film.[5–10] The potential of using SPs to manipulate light in the subwavelength spaces opens up a multitude of new possibilities for subwavelength lithography,[3,4,11] optical data storage,[12,13] microscopy, and biophotonics.[14,15] SPs exhibit very unique dispersive behavior, which could lead to the optical lithography at a resolution beyond the diffraction limit. The dispersion relation of SPs at an interface of dielectric metal is given by[16] $k_{SP} = \sqrt{\varepsilon_1 \varepsilon_m / (\varepsilon_1 + \varepsilon_m)}(2\pi/\lambda_0)$ where k_{SP} is the transverse wave number of the eigenmode of the SPs, λ_0 is the light wavelength in vacuum, and ε_1 and ε_m are the permittivities of the dielectric and metal layers, respectively. In order to achieve higher resolution, it is essential to access high wavenumbers of SPs which correspond to short wavelengths of SPs. According to the SP dispersion curve, the short modal wavelengths of SPs can be accessed at the SP frequency when the

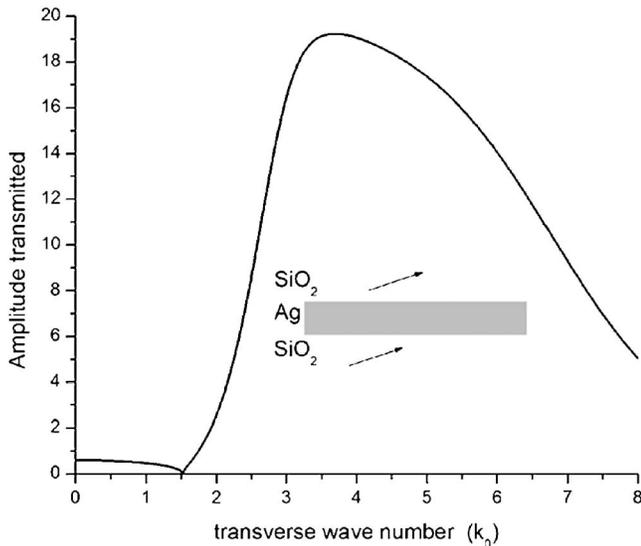[a] Author to whom correspondence should be addressed; electronic mail: xzhang@me.berkeley.edu

FIG. 1. Transmitted amplitude of varied wave numbers (transfer function) through a 40 nm thick silver slab for *p*-polarized waves.

FIG. 2. (a) Simulated amplitude of *E*-field at the cross section of silver hole array; silver film thickness 40 nm, hole diameter 20 nm, periodicity 40 nm. (b) Silver hole array with titanium adhesion layer (3 nm) at the same condition as (a).

localized SP (LSP) condition ($\varepsilon_m = -\varepsilon_1$) is satisfied.[16] As a result, it is possible to resolve very small feature patterns with very high intensity. Silver is chosen since it is known as the superior low loss material and its LSP condition ($\varepsilon_m = -\varepsilon_1$) can be satisfied in UV wavelength range. For example, silver film at 365 nm wavelength (*I*-line) has the permittivity of $\varepsilon_m = -2.5 + 0.69i$ as interpolated from Ref. 17, which requires the refractive index (n) of the surrounding dielectric medium ~ 1.58 to satisfy the condition.

In order to estimate the resolution limit of the proposed lithography method, the transmission amplitude of each wave-number component is considered. Here, we use the transfer function of a nonperforated homogeneous silver film to understand the optical transmission through the mask qualitatively. The amplitude transmitted (*H*-field) at $\lambda_0 = 365$ nm for *p*-polarized waves as a function of transverse wavenumber (k) through a 40 nm thick silver slab shows that evanescent waves can be transmitted with a large amplitude for the wave numbers between $2.5k_0$ and $8k_0$ (where $k_0 = 2\pi/\lambda_0$), as shown in Fig. 1. Consequently, any grating with the periodicity corresponding to the wave numbers within that range can excite the SPs efficiently leading to the potential of lithography at deep subwavelength resolution. It should be noted that the wave number is inversely proportional to the wavelength of SPs where the lithographic resolution is approximately half of the wavelength. Roughly, this result predicts that feature size as small as 20 nm ($\lambda_0/16$; corresponding to half of the SP wavelength $\lambda_0/8$ at the wave number of $8k_0$) could be practically achieved. Recently the "superlensing"[18] concept—high-resolution imaging through a silver slab—was experimentally demonstrated.[19] In this experiment, a one-dimensional grating pattern (60 nm lines with 120 nm period) perforated on a chromium layer as an object was imaged through a silver slab (superlens) and recorded in photoresist on the other side of the silver. The result strongly c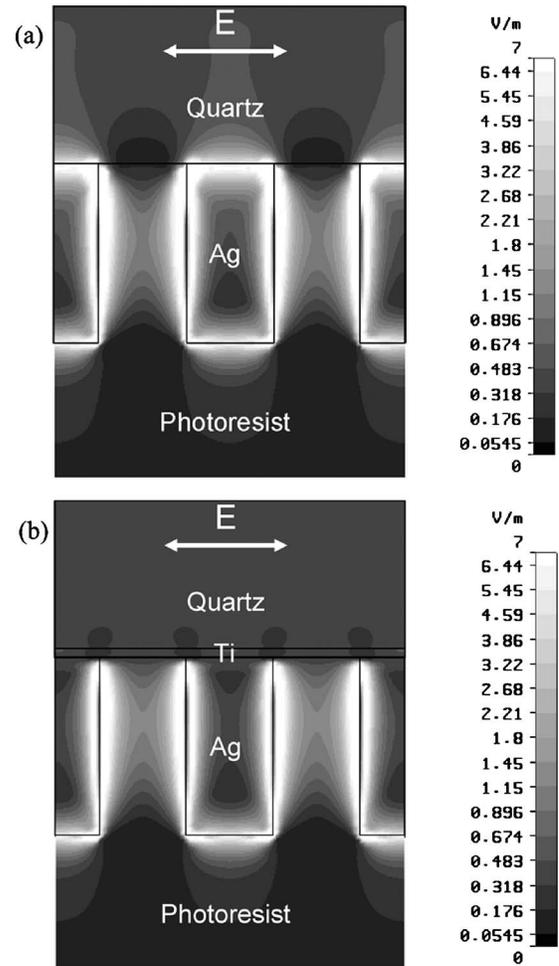onfirms the high transmission of the large evanescent wave-number components of evanescent field through the silver slab as described in the transfer function (Fig. 1). However, the above analytical investigation is based on the optical transmission property through a nonstructured homogeneous silver film. To understand the transmitted field profile through a structured silver mask would require further theoretical and numerical studies.

A number of numerical simulations of the lithography at SP resonant frequency were conducted to further investigate the field transmitted through the structured silver mask. The three-dimensional simulations were done by using commercial finite-difference time-domain (FDTD) software (Microwave Studio). The simulated structure is a 2 by 2 hole array perforated on silver film where the boundary conditions along x and y are set to be periodical. The hole diameter, periodicity, and silver layer thickness are 20, 40, and 40 nm, respectively. The refractive indices (n) of the quartz substrate, photoresist, and silver used in the simulation are 1.48, 1.57, and $0.218 + 1.596i$, respectively. The incident plane wave illumination is linearly polarized along the x direction with an *E*-field amplitude of 1 V/m. Figure 2(a) shows the
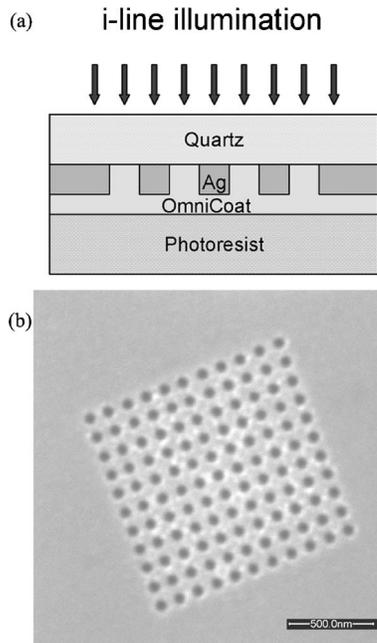
(a)   i-line illumination

(b)

FIG. 3. (a) Schematic of lithography setup using a silver mask. (b) Scanning electron microscope image of a silver hole array fabricated by FIB; silver film thickness 40 nm, hole diameter 60 nm, periodicity 120 nm.
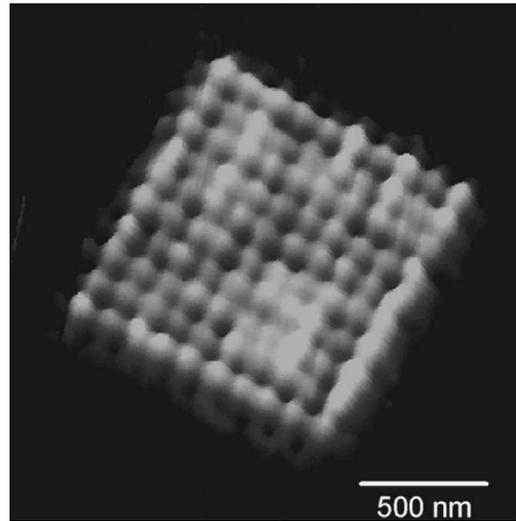

FIG. 4. AFM image of an exposure pattern on 120 nm period, where the hole size of 60 nm, the silver film thickness of 40 nm, the spacer layer thickness of 15 nm, and the exposure dose of 80 mJ/cm^2.

simulated E-field amplitude at the cross-sectional view at the center of the holes. It should be emphasized that the E-field amplitude is strongly enhanced on the silver film by a factor of 7 compared to that of the incident while the E-field amplitude upon the holes is much weaker. This implies the contribution of the short wavelengths of SPs at the SP resonant frequency where features as small as 20 nm can be resolved.

III. NANOLITHOGRAPHY EXPERIMENT

The mask designed for lithography at the wavelength of 365 nm is composed of a silver layer perforated with a 2-D periodic hole array pattern and sandwiched between quartz and OmniCoat (MicroChem) layers (refractive indices are 1.48 and 1.57, respectively) as schematically shown in Fig. 3(a). The surface roughness of silver film is a critical parameter from the practical viewpoint, since short wavelengths of SPs are strongly scattered on a rough surface. Here, we reduced the surface roughness of silver film by adding an adhesion layer of titanium between the silver and the quartz substrate. Owing to the better adhesion, the surface roughness of the silver film is significantly reduced from 3 nm rms to 1 nm rms over 10 μm $\times$ 10 μm square area. This configuration enables us to fabricate small features on silver film with significantly small surface roughness as shown in Fig. 3(b). A FDTD numerical study suggested that the E-field profile on the exit side of silver mask is not perturbed by the thin titanium layer [Fig. 2(b)] as compared to the simulation result without the adhesion layer of titanium [Fig. 2(a)].

In the lithography experiment, the plasmonic mask is prepared as follows: a 3 nm titanium film is deposited by an E-beam evaporator on a quartz substrate, and next a 40 nm thick silver film is deposited on the titanium adhesion layer.

Hole arrays with a variety of dimensions are fabricated on silver film by focused ion-beam (FIB) milling (FEI Strata 201 XP). Subsequently, a 15 nm thick spacer layer of Omni-Coat™ is spun on the patterned silver film. To demonstrate the resolution of the proposed method, a negative near UV photoresist (SU-8) is directly spun on the top of the spacer layer and polymerized on the mask. This configuration can eliminate the gap variation between the mask and the photoresist in the lithography process. The sample is exposed using a filtered mercury lamp with a radiation peak at 365 nm. After the development, the topography of the recorded features is characterized by an atomic force microscope (AFM, Dimension 3100, Veeco).

The AFM image in Fig. 4 is an exposure result obtained from a mask that consists of an array of holes 60 nm in diameter and 120 nm in period. The exposure time is 10 s, corresponding to the exposure dose of 80 mJ/cm^2 at the mask. The exposure result shows the remaining features of negative photoresist SU-8 on the area corresponding to the silver film in between the holes. This result implies the strong field is located on the silver surface rather than the holes of the mask and it is in good agreement with the simulation study. Features as small as 60 nm (equivalent to $\lambda_0/6$) have been obtained. It should be noted that the fidelity of the transferred pattern is significantly high due to the particularly short propagation length of SPs in this case ($<$20 nm). It should be noted that the resolution demonstrated in the lithography experiment was limited mainly by the resolution of the mask. Further demonstration of higher resolution is still ongoing. Furthermore, as suggested in the transfer function,[19] the silver layer is capable of transferring a broad spectrum of the wave numbers from $2k_0$ to $8k_0$, which implies the method presented in this paper can be further applied for patterning the arbitrary geometry with the ultimate resolution at $\lambda/16$.

IV. CONCLUSIONS

In conclusion, we presented a systematic study of high-resolution near-field optical lithography at SP resonant frequency. By accessing shorter modal wavelengths of SPs at the resonant frequency, higher lithographical resolution can be obtained while using a conventional UV light source. The FDTD simulation indicated a strongly enhanced near-field profile with the spatial confinement down to the order of 20 nm. With the success in optimizing the mask fabrication process, we then conducted the lithography experiment. The result revealed that a sub-diffraction-limited field profile at a half-pitch resolution at 60 nm ($\lambda/6$) can be achieved using a 2-D hole array sliver mask.

ACKNOWLEDGMENTS

[1] A. K. Bates, M. Rothschild, T. M. Bloomstein, T. H. Fedynyshyn, R. R. Kunz, V. Liberman, and M. Switkes, IBM J. Res. Dev. **45**, 605 (2001).
[2] M. M. Alkaisi, R. J. Blaikie, and S. J. Mcnab, Microelectron. Eng. **53**, 237 (2000).
[3] W. Srituravanich, N. Fang, C. Sun, Q. Luo, and X. Zhang, Nano Lett. **4**, 1085 (2004).
[4] W. Srituravanich, N. Fang, S. Durant, M. Ambati, C. Sun, and X. Zhang, J. Vac. Sci. Technol. B **22**, 3475 (2004).
[5] T. W. Ebbesen, H. J. Lezec, H. F. Ghaemi, T. Thio, and P. A. Wolff, Nature (London) **391**, 667 (1998).
[6] T. Thio, H. F. Ghaemi, H. J. Lezec, P. A. Wolff, and T. W. Ebbesen, J. Opt. Soc. Am. B **16**, 1743 (1999).
[7] A. Krishnan, T. Thio, T. J. Kim, H. J. Lezec, T. W. Ebbesen, P. A. Wolff, J. Pendry, L. Martin-Moreno, and F. J. Garcia-Vidal, Opt. Commun. **200**, 1 (2001).
[8] A. Dogariu, A. Nahata, R. A. Linke, L. J. Wang, and R. Trebino, Appl. Phys. B: Lasers Opt. **74**, S69 (2002).
[9] L. Salomon, F. Grillot, A. V. Zayats, and F. V. de Fornel, Phys. Rev. Lett. **86**, 1110 (2001).
[10] W. L. Barnes, A. Dereux, and T. W. Ebbesen, Nature (London) **424**, 824 (2003).
[11] L. Xiangang and T. Ishihara, Appl. Phys. Lett. **84**, 4780 (2004).
[12] K. Tanaka, H. Hosaka, K. Itao, M. Oumi, T. Niwa, T. Miyatani, Y. Mitsuoka, K. Nakajima, and T. Ohkubo, Appl. Phys. Lett. **83**, 1083 (2003).
[13] E. X. Jin and X. Xu, Appl. Phys. Lett. **86**, 648 (2005).
[14] S. A. Maier, M. L. Brongersma, P. G. Kik, and H. A. Atwater, Phys. Rev. B **65**, 193408 (2002).
[15] Q.-H. Wei, K.-H. Su, S. Durant, and X. Zhang, Nano Lett. **4**, 1067 (2004).
[16] H. Raether, *Surface Plasmons on Smooth and Rough Surfaces and on Gratings* (Springer, Heidelberg, 1988), pp. 9–30.
[17] P. B. Johnson and R. W. Christy, Phys. Rev. B **6**, 4370 (1972).
[18] J. B. Pendry, Phys. Rev. Lett. **85**, 3966 (2000).
[19] N. Fang, H. Lee, C. Sun, and X. Zhang, Science **308**, 534 (2005).